Tunneling and Intersubband Coupling in Ultra-Thin Body Double-Gate MOSFETs

Viktor Sverdlov [(1)], Andreas Gehring [(2)], Hans Kosina [(1)], and Siegfried Selberherr [(1)]

(1) Institute for Microelectronics, TU Vienna, Gusshausstr. 27–29, A-1040 Vienna, Austria.
(2) AMD Saxony LLC & Co. KG, Wilschdorfer Landstrasse 101, D-01109 Dresden, Germany
sverdlov@iue.tuwien.ac.at, andreas.gehring@amd.com, kosina@iue.tuwien.ac.at

Abstract:

Deca-nanometer double-gate MOSFETs is studied using a quantum Wigner Monte Carlo approach, including electron-phonon scattering. Intersubband coupling elements are explicitly calculated and proven to be small in double-gate MOSFETs. This allows quantum transport simulations to be analyzed using decoupled subbands. For long gate length the semi-classical result is recovered. An increasing tunneling component of the drain current with decreasing gate length is obtained. The results clearly show the importance of scattering for gate lengths as short as 25 nm. Performance enhancement due to ballistic transport can thereby be estimated.

1. Introduction

Double-gate transistors are an attractive option to improve the performance of logic devices and overcome some of the difficulties encountered in further downscaling of bulk MOS field-effect transistors into the deca-nanometer regime [1]. When the channel length is reduced below approximately 25 nm, quantum effects such as direct source-to-drain tunneling through the barrier start affecting the device characteristics. Frequently, ballistic transport is assumed which allows the device to be simulated using pure quantum-mechanical approaches [2, 3]. However, with carrier mean free paths in the range of several nanometers [4], scattering-limited transport may still be dominant. A precise theory of ultrascaled double-gate MOSFETs (DGMOSFETs) must therefore properly account for an interplay between the quantum nature of carrier propagation inside the channel and scattering processes. The nonequilibrium Green's functions method addresses the problem in the most consistent and complete way. Due to its computational complexity, the method is frequently used in its reduced coherent version, which is equivalent to the solution of the Schrödinger equation with open boundary conditions. Introduction of scattering into the method requires the knowledge of the corresponding self-energies and complicates computations significantly [5].
An alternative approach is based on the Wigner function formalism. It incorporates quantum mechanical effects in terms of a quantum scattering operator [6]. An advantage of the Wigner function approach is that it allows to account for all scattering mechanisms via the Boltzmann scattering integral. It makes possible a development of a rigorous transport model with both quantum interference phenomena and the coherence-breaking scattering mechanisms. The Wigner function formalism treats the scattering and quantum mechanical effects on equal footing through the corresponding scattering integrals. The remaining collision-free propagation of the carriers is described by the Liouville operator acting on the Wigner function and is similar to that of the Boltzmann equation. It prompts for a solution of the Wigner equation by a Monte Carlo algorithm, in analogy to the solution of the Boltzmann equation. Such a program was recently realized in [6, 7]. It was pointed out that, because the kernel of the quantum scattering operator being not positively defined, the numerical weight of a particle trajectory increases rapidly, and the numerical stability of a trajectory-based Monte Carlo algorithm becomes a critical issue. A multiple trajectories method was recently suggested [6] in order to overcome the difficulty. In this algorithm the problem of a growing statistical weight of a single trajectory is addressed by creating of an increasing number of trajectories with constant weights, which may assume positive and negative values. Being formally equivalent to the former method, the algorithm allows the annihilation of trajectories with similar statistical properties, introducing a possibility to control the number of trajectories.

Size quantization effects in the ultra-thin Si body of DG-MOSFETs lead to the formation of two-dimensional subbands. Under nonequilibrium conditions, when the drain-to-source and gate voltages are applied, the subbands become quantum mechanically coupled, due to a simultaneous non-separable dependence of the conduction band in the channel on both lateral and transversal coordinates. A common approximation used in simulations of DGMOSFETs is an adiabatic subband decomposition method, where it is assumed that the intersubband coupling due to non-adiabatic effects should be small. A good agreement between the results of simulations using the space-mode approach and the full-scale simulations [3] indicates that the subband decomposition may be a good approximation. However, recent studies have shown that even when the subband coupling is expected to be strong, results of current characteristic simulations using both of the foregoing approaches coincide within 10% [8]. This suggests that the coupling elements have to be evaluated in order to decide on their actual importance.

In this paper we report on mixed semiclassical - quan-

0-7803-9205-1/05/$20.00 ©2005 IEEE

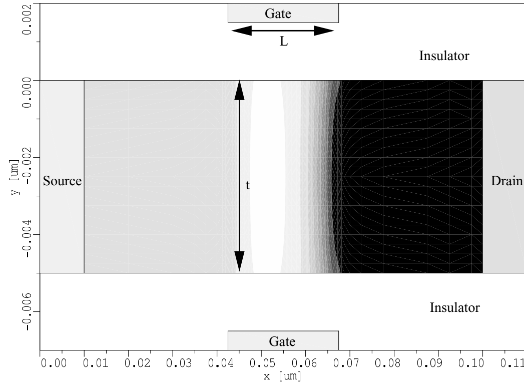

Figure 1: Sketch of the 25 nm gate length doublegate MOSFET structure. The contour plot shows the potential profile of the conduction band in the channel at the drainsource bias of 0.3 V and gate voltage 0.0 V.

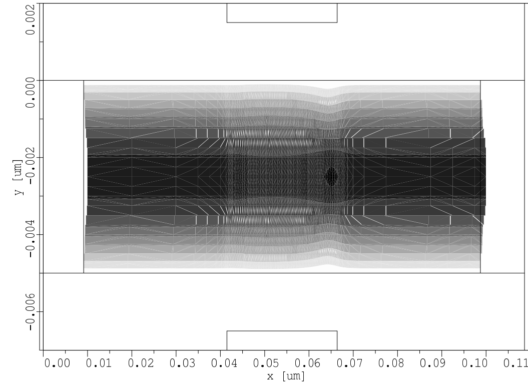

Figure 2: Profile of the lowest subband wave function determined by (1). The parameters are the same as in Fig. 1.

tum Wigner Monte Carlo simulations of a doublegate architecture which represents an ideal structure of recently manufactured doublegate devices [9]. In order to obtain a realistic potential profile in the presence of dissipative scattering processes, we use the MINIMOS-NT simulator [10] in the driftdif fusion mode, with a quantum correction potential introduced in order to account for a proper carrier density behavior at the channel boundaries selfconsistently . We then evaluate the subband profiles and the wave functions. The intersubband coupling elements in DGMOSFETs under nonequilibrium conditions when sourcedrain bias is applied are explicitely calculated. It is shown that in ultrascaled DGMOSFETs the coupling terms are small as compared to the thermal energy and/or intersubband splitting, and the subband decomposition turns out to be an excellent approximation. The Wigner function based Monte Carlo simulations of the sourcedrain current including tunneling and dissipative processes in each subband are performed.

2. Transport Model and Results

The DGMOSFET is schematically shown in Fig. 1. An undoped Si semiconductor channel of thickness t is connected to the heavily doped source and drain contacts, with the dopant concentration set to $5 \times 10^{19}\,\mathrm{cm}^{-3}$. The doping profile is chosen to be abrupt. Metal gates of length L with midgap work function are assumed. Gate electrodes are separated from the channel by thin layers of silicon dioxide. In the simulations the gate length L varies from 10 to 60 nm. The silicon film thickness t is in the range between 3 and 20 nm. The system is assumed to be infinite in z direction, such that the transversal motion in z direction is described by the conserved transversal momentum p_z and may be separated.

Due to the small silicon body thickness, the transversal carrier motion in y direction is quantized. The electron spectrum is split into well defined two dimensional subbands. Each subband is characterized by the transversal wave function $\psi_n(y,x)$. The subband wave functions are defined from the effective mass equation:

$$\left[-\frac{\hbar^2}{2m_y}\frac{\partial^2}{\partial y^2}+U(y,x)\right]\psi_n(y,x)=\mathcal{E}_n(x)\psi_n(x,y), \quad (1)$$

where $U(y,x)$ is the selfconsistent potential energy in the channel, and m_y is the effective mass in y direction. The contour plot of the lowest subband wave function calculated at different position x of the chanel crosssection is shown in Fig. 2. Lowest subband profiles for a MOSFET with L =25 nm and $t = 5$ nm is shown in Fig. 3. Note that due to the dependence of the longitudinal coordinate x still present in the potential profile $U(y,x)$, the eigenfunctions $\psi_n(y,x)$ and eigenenergies $\mathcal{E}_n(x)$ depend on x. Because of this dependence the subbands defined by $\psi_n(y,x)$ are not completely separable.

The intersubband coupling elements are

$$\delta H_{nm}(x)=\sum_{m\neq n}\left(S_{nm}(x)\frac{\partial}{\partial x}+D_{nm}(x)\right), \quad (2)$$

where the coefficients $S_{nm}(x)$ and $D_{nm}(x)$ are defined as

$$S_{nm}(x)=-\frac{\hbar^2}{m_x}\int dy\psi_n(y,x)\frac{\partial}{\partial x}\psi_m(y,x),$$

$$D_{nm}(x)=-\frac{\hbar^2}{2m_x}\int dy\psi_n(y,x)\frac{\partial^2}{\partial x^2}\psi_m(y,x).$$

The potential profile inside the channel of DGMOSFETs calculated with MINIMOS-NT is shown in Fig. 1. A drain-source voltage of 0.3 V and a gate bias of 0 V were applied. The equipotential lines develop high curvatures at the drain end of the channel between the gates.

The strong x dependence of the wave function is seen in the same channel region (Fig. 2).

The elements $D_{nm}(x)$ and $S_{nm}(x)$ of the coupling Hamiltonian are shown in Fig. 4 and Fig. 5, for several values of silicon thicknesses t and gate lengths L. As expected, all the coupling elements are substantially different from zero in the narrow channel segment where the channel potential and the transversal wave functions feature a strong longitudinal gradient.

Diagonal and offdiagonal coupling elements show a different behavior as a function of silicon body thickness t.

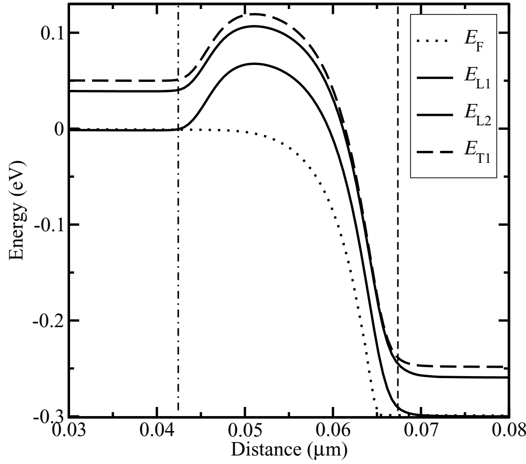

Figure 3: Potential profile of three lowest subbands $\mathcal{E}_n(x)$ and the quasi-Fermi $\mathcal{E}_F$ level in L =25 nm and t =5 nm MOSFET. Only the lowest subband is substantially occupied with carriers and thus participates in transport.

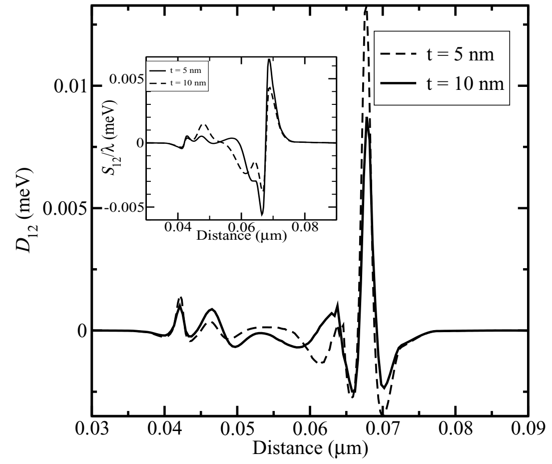

Figure 4: Off-diagonal part $D_{12}(x)$ of the coupling Hamiltonian calculated for gate length $L = 25$ nm, for two values of the silicon body thickness t. The coupling increases slightly as the thickness is decreased. Inset: off-diagonal term $S_{12}(x)$, normalized to the thermal length $\lambda = \sqrt{2m_x k_B T}/\hbar$, for two values of body thickness.

The diagonal contribution $D_{nn}(x)$ is rapidly decreasing when the thickness of the silicon film shrinks, whereas both contributions S_{nm} and D_{nm} to the off-diagonal part show an opposite tendency to grow slightly when the body thickness is reduced (Fig. 4 and inset). For fixed silicon film thickness, as the gate length L is decreased, the diagonal and off-diagonal contributions show similar tendency to increase. However, as one can see from Fig. 5, the L dependence of D_{nn} is quite weak, since the absolute increase is only about 15% when the channel length is reduced from 50 nm to 15 nm.

As can be seen from comparing Fig. 3 and Fig. 4, the absolute value of the off-diagonal coupling elements $D_{nm}(x)$ and $S_{nm}(x)/\lambda$, where $\lambda = \sqrt{2m_x k_B T}/\hbar$ is the thermal wavelength, is of the order of 10^{-2} meV. This value is extremely small compared to other characteristic energies such as $k_B T$ or the subband quantization energy. It is thus justified to neglect the off-diagonal coupling $\delta H_{nm}(x)$ for the DGMOSFETs under consideration. The diagonal contribution $D_{nn}(x)$ can be absorbed into $V(x)$ describing the potential profile of the n-th subband:

$$V(x) = \mathcal{E}_n(x) + D_{nn}(x). \quad (3)$$

Introducing the Wigner function $f_n(x,p,t)$ for each subband n and following the procedure outlined in [6], we obtain the one-dimensional Wigner equation for $f_n(x,p,t)$. The potential operator of the one-dimensional Wigner equation is given by the usual convolution integral [11], where the potential energy of electrons $V(x)$ is defined by (3). An additional convergence improvement may be achieved by an appropriate choice of a separation of the subband potential profile into a classical part and a quantum mechanical contribution [11] by choosing a smooth classical component as an output of a low-pass filter with the cut-off wave number $q_c \ll 2\pi/\Delta x$, where Δx is the grid step.

The Wigner function based Monte Carlo method was applied to DGMOSFETs with gate lengths of 60, 25, 15, and 10 nm and silicon film thicknesses of 20, 10, 5, and 3 nm, respectively, at a gate bias of 1.0 V. The carrier concentrations in the different devices at a drain bias of 0.6 V are shown in Fig. 6. Although the difference is small in absolute numbers, it is significant that for the 10 nm gate length device the Wigner simulation predicts carrier concentrations in the channel which are almost 50% higher than predicted by the classical simulation.

The output characteristics of the 60, 25, and 10 nm devices are shown in Fig. 7. At 60 nm, the Wigner calculations reproduce the classical results, while they predict higher currents at smaller gate lengths. This is due to source-drain tunneling which, in contrast to the classical simulations, is properly accounted for by the Wigner function based Monte Carlo simulations.

3. Conclusions

The Wigner function based Monte Carlo method coupled with the classical self-consistent MINIMOS-NT simulator is used to analyze the interplay between the coherent carrier motion and dissipative scattering effects. This procedure allows a direct comparison of semi-classical and quantum transport results. The method is used to account for the tunneling current in ultra-scaled double-gate MOSFETs. Intersubband coupling elements are explicitely computed and are proven to be small. The subband decomposition is shown to be an excellent approximation in DGMOSFETs. Devices of different gate lengths have been studied. Scattering substantially reduces the on-current compared to the ballistic case. The simulations reproduce the semi-classical results for the long channel device and predict a significant source-to-drain tunneling component in the drain current at very short gate lengths.

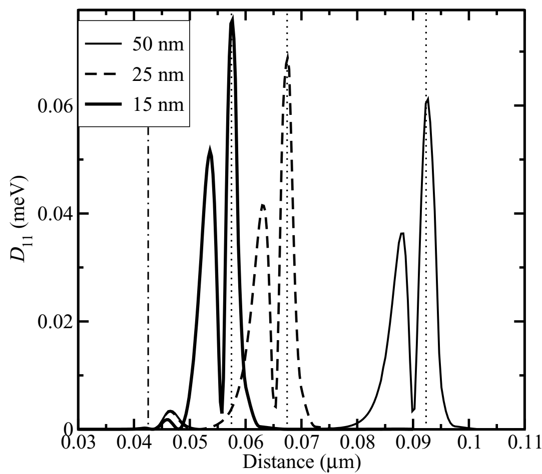

Figure 5: Diagonal part $D_{11}(x)$ of the perturbation Hamiltonian calculated for silicon body thickness t =5 nm, for three different gate lengths. The dashed-dotted line shows the left edge and dotted lines the right edge of the gates, respectively.

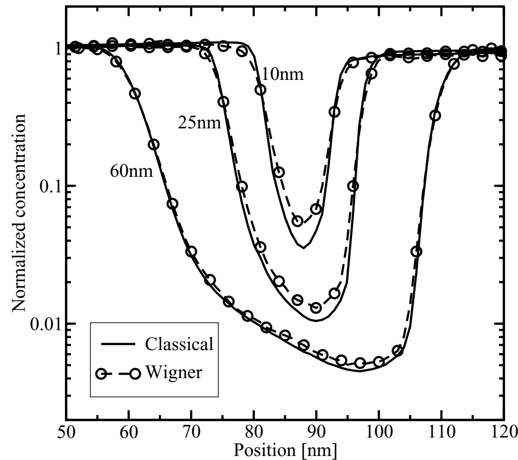

Figure 6: The carrier concentrations in the 10 nm, the 25 nm, and the 60 nm gate length device at 0.6 V drain bias for the classical and the Wigner Monte Carlo simulations.

Acknowledgment

This work has been partly supported by the Austrian Science Fund FWF, project P17285-N02, and the European Commission, project SINANO IST-506844.

References:

[1] J.-P. Colinge. Multiple-Gate SOI MOSFETs. *Solid-State Electron.*, 48:897–905, 2004.

[2] M. Lundstrom and Z. Ren. Essential Physics of Carrier Transport in Nanoscale MOSFETs. *IEEE Trans.Electron Devices*, 49(1):133–141, 2002.

[3] R. Venugopal, Z. Ren, S. Datta, M. S. Lundstrom, and D. Jovanovic. Simulation of Quantum Transport in Nanoscale Transistors: Real versus Mode-Space Approach. *J.Appl.Phys.*, 92(7):3730–3739, 2002.

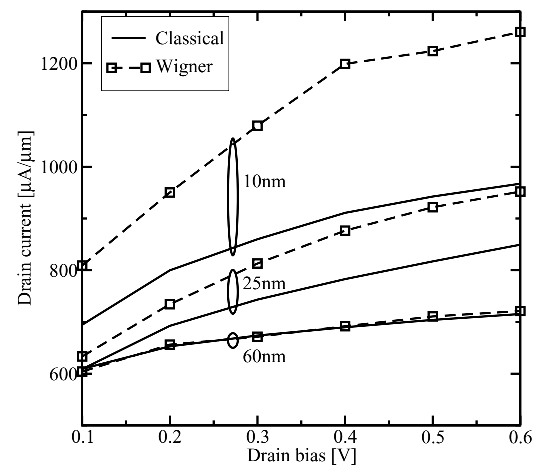

Figure 7: Output characteristics of the 10 nm, the 25 nm, and the 60 nm gate length device using classical and Wigner Monte Carlo. The additional source-to-drain tunneling current component is clearly visible for the short-channel devices.

[4] C. Jungemann, N. Subba, J.-S. Goo, C. Riccobene, Q. Xiang, and B. Meinerzhagen. Investigation of Strained Si/SiGe Devices by MC Simulation. *Solid-State Electron.*, 48(8):1417–1422, 2004.

[5] A. Svizhenko and M. P. Anantram. Role of Scattering in Nanotransistors. *IEEE Trans.Electron Devices*, 50:1459–1466, 2003.

[6] H. Kosina, M. Nedjalkov, and S. Selberherr. A Monte Carlo Method Seamlessly Linking Quantum and Classical Transport Calculations. *J. Computational Electronics*, 2(2–4):147–151, 2002.

[7] L. Shifren, C. Ringhofer, and D. K. Ferry. A Wigner Function-Based Quantum Ensemble Monte Carlo Study of a Resonant Tunneling Diode. *IEEE Trans.Electron Devices*, 50(3):769–773, 2003.

[8] R. Venugopal, S. Goasguen, S. Datta, and M. S. Lundstrom. Quantum Mechanical Analysis of Channel Access Geometry and Series Resistance in Nanoscale Transistors. *J.Appl.Phys.*, 95(1):292–305, 2004.

[9] S. Harrison, O. Coronel, F. Leverd, R. Cerutti, R. Pala, D. Delille,S. Borel, S. Jullian, R. Pantel, S. Descombes, D. Dutartre, Y. Morand, M.P. Samson, A. Talbot, A. Villaret, S. Monfray, P. Mazoyer, J. Bustos, H. Brut, A. Cros, D. Munetanu, J.-L. Autran, T. Skotnicki. Highly Performant Double Gate MOSFET Realized with SON Pocess. In *Proc. Intl. Electron Devices Meeting*, pages 18.6.1–18.6.4, Piscataway, NJ, 2003. IEEE Press.

[10] Institut für Mikroelektronik, Technische Universität Wien, Austria. Minimos-NT 2.1 User's Guide. http://www.iue.tuwien.ac.at/software/minimos-nt , 2004.

[11] A. Gehring and H. Kosina. Wigner-Function Based Simulation of Quantum Transport in Scaled DG-MOSFETs Using the Monte Carlo Method. *J.Computational Electronics*, in print.